Seminar series nr 286

# Finding a method for simplified biomass measurements on Sahelian grasslands

**Elise Palm**

2013
Department of Physical Geography
and Ecosystem Science
Lund University
Sölvegatan 12
S-223 62 Lund
Sweden

Elise Palm (2013). Finding a method for simplified biomass measurements on Sahelian grasslands
Master degree thesis, 30 credits in Physical Geography and Ecosystem Science
Department of Physical Geography and Ecosystem Science, Lund University

# Finding a method for simplified biomass measurements on Sahelian grasslands

Elise Palm

**Master's Degree Thesis, 30 credits in**
Physical Geography and Ecosystem Analysis
**Supervisor:**
Jonas Ardö
Department of Physical Geography and Ecosystem Science
Lund University, Sweden, 2013

## Acknowledgements

There are many who have been helpful and supportive during the course of both the field work and the writing of this thesis. I would like to thank my supervisor Jonas Ardö for helping and coaching me through this work. Moreover, my warmest thanks to:

"The Danish crew" consisting of Rasmus Fensholt, Bo Holm-Rasmussen and Marc Ridler,

"The Dakar crew" consisting of Cheikh Mbow, Idrissa Guiro and Doudou Diop, and

"The ISRA crew" consisting of a lot of people, but most namely Monsieur and Madame Sane and Fatou.

Last but not least: thanks to my family and friends for all of your support!

## Abstract

Traditional measurements for determination of aboveground biomass (AGB) are widely used in ecological studies. However, they are labor demanding and time consuming, why this study performed on a grassland in Senegal has focused on finding a simplified AGB estimation method that could be applied on larger areas in the Sahel. The brightness values in the visible spectral range of digital camera images (DCIs) have been tested for correlation with traditional AGB using three already established indices leading to $r^2$ values of 0.57, 0.56 and 0.43 (all attained p=<0.0001) when including all four measurement occasions, and $r^2$ values of 0.63, 0.61 and 0.51 (p=<0.0001) when excluding the last occasion, which had a high amount of yellowing grasses. Some of the DCIs were also visually interpreted after performing an unsupervised image classification in two groups. This did not seem to reveal any new insights in the usage of DCIs as estimation of AGB. Grass height, on the other hand, showed a higher correspondence with AGB ($r^2$=0.79 and p<=0.0001 for all occasions and $r^2$=0.70 and p<=0.0001 when excluding the last occasion). In addition to the higher correlation, measuring grass height is also the least expensive and the quickest of the methods investigated in this study and can hopefully be applied on larger areas by local farmers.



**Keywords:** biomass, grasslands, Sahel, digital camera images, LAI



## Sammanfattning

Traditionella mätningar av biomassa används ofta i ekologiska studier. Då denna typ av mätningar är arbetsintensiva och tidskrävande har denna studie utförd på en gräsmark i Senegal fokuserat på att hitta en metod som är lättare att använda och som kan användas över större områden i Sahel. Pixelvärdena i den synliga delen av spektret från digitala kamerabilder testades för korrelation mot biomassa i fält genom att applicera tre olika etablerade index på bilderna. Detta ledde till $r^2$-värden som uppgick till 0.57, 0.56 och 0.43 (alla erhöll p-värden under 0.0001) när alla fyra mätningstillfällen användes. När det sista mätningstillfället, som innehöll en hög andel gult gräs, exkluderades erhölls $r^2$-värden på 0.63, 0.61 och 0.51 (p<=0.0001). Vissa digitala kamerabilder tolkades visuellt efter att ha utfört en oövervakad klassificering i två grupper. Detta verkade inte ge några nya insikter vid uppskattning av biomassa med hjälp av digitala kamerabilder. Gräshöjd uppvisade däremot en högre korrelation med biomassa (r2=0.79 och p<=0.0001 för alla fyra tillfällen och $r^2$=0.70 och p<=0.0001 då det sista tillfället exkluderades). Utöver den högre korrelationen är mätningar av gräshöjd den billigaste och snabbaste av de metoder som undersökts i denna studie. Förhoppningsvis kan denna metod också utföras över stora områden av lokala bönder.

# Contents

## List of abbreviations

AGB – Above ground biomass
DN – Digital number
DOY – Day of year
ESA – European Space Agency
JPEG – Joint photographic experts group
MERIS - Medium Resolution Imaging Specrometer
MODIS – Moderate Resolution Imaging Spectroradiometer
NASA – National Aeronautics and Space Administration
NDGI – Normalized difference greenness index
NDVI – Normalized difference vegetation index
NIR – Near infra-red
PAR – Photosynthetically active radiation
RGB – The three dimensional color space of red, green and blue
VF – Vegetation Fraction

# 1. Introduction

The onset of this project was brought up by a wish to facilitate biomass measurements on Sahelian grasslands. It is a collaboration between the University of Copenhagen in Denmark, the University of Dakar in Senegal and Lund University in Sweden. These universities already carry out ecological research in this area. Furthermore, the Swedish International Development Cooperation Agency (SIDA) supported the project with a scholarship within the framework of their Minor Field Study (MFS) program.

## 1.1 Background

Traditional biomass measurements are considered the most reliable method for determining aboveground biomass (AGB) (Desalew et al., 2010). However, they are extremely labor demanding and time consuming; including cutting of biomass in field, followed by drying and weighing of biomass in laboratories.

As an alternative, or aid, to traditional measurements of AGB, satellite remote sensing has been explored to provide management information for larger areas of land at a lower cost (Vanamburg et al., 2005). But limitations of satellite remote sensing of vegetation include e.g. image contamination by aerosols and clouds, unwanted effects of changes in viewing angle (Richardson et al., 2007) and inability to separate vegetation from soil backgrounds (Vanamburg et al., 2005). As a result, biomass estimation by satellites is an area in need of reference data, which might be used to aid in the analysis and interpretation of remotely sensed data, calibrate a sensor and/or verify and evaluate information extracted from remote sensing data (Lillesand et al., 2008).

Optimally, flux tower measurements are used to validate e.g. MODIS primary productivity estimates (EROS, 2012). The towers measure NEE (Net Ecosystem Exchange) of $CO_2$ between the biosphere and the atmosphere. From these measurements, NPP (Net Primary Productivity) and GPP (Gross Primary Productivity) can be estimated. This, in turn, is used to validate MODIS-derived NPP and GPP. However, the sparse distribution of towers cause challenges in the attempt to validate satellite products as there are very large areas lacking reference data (Reeves et al., 2006).

The methods for estimating grassland NPP, which is defined as the new plant material that is produced annually per area unit (Chapin et al., 2002), generally include biomass measurements in some way. The three most commonly used estimates of NPP are peak, live AGB, peak (live plus dead) AGB and the difference between maximum and minimum AGB (Scurlock et al., 2002). Hence, biomass is needed to estimate ground NPP, and ground NPP is needed to calibrate satellite derived NPP.

In this study, performed in Dahra, Senegal, images from a digital camera have been used to investigate grass greenness from the start to the peak of the growing season. In addition, measurements of grass height were performed. Results obtained from the images and from the grass height measurements were compared to biomass to examine whether any relationships existed. A good correspondence between biomass and the collected data could contribute to a facilitation of biomass estimation covering larger areas of Sahelian grasslands and could maybe even offer possibilities to calibrate satellite derived data for biomass estimations in the future. A successful result could also complement already existing traditional biomass measurements.

An ideal method for estimation of aboveground dry biomass should:
(a) be accurate and objective
(b) be cost efficient
(c) place minimum demands on field time.

## 1.2 Biomass

Biomass is defined as the total amount of living vegetation in e.g. a habitat or a sample (Chapin et al., 2002) and is a measure of vegetative growth. Biomass measurements and estimations are applied in several disciplines, such as carbon cycle studies and natural resource assessments. Briefly, the solar energy, fixed by chlorophyll in photosynthesis, supports plant growth and maintenance by converting $CO_2$ and $H_2O$ to carbohydrates (Chapin et al., 2002). The total radiation absorbed by a plant between wavelengths 0.4 and 0.7 µm quantifies the energy available for NPP (Rautiainen et al., 2010).

Plants adjust the components of photosynthesis in order to make $CO_2$ diffusion and biochemistry equally limit photosynthesis – an adjustment that is altered by stomatal conductance; the flux of water vapor or $CO_2$ for a given concentration gradient. Through the leaf stomata, plants gain $CO_2$ from the atmosphere and transpire water vapor and oxygen ($O_2$). Once inside the plant, $CO_2$ dissolves in water that covers the cell walls and is then transferred into the cells. This water eventually evaporates and is transpired through the stomata out to the atmosphere. In extension, this means there is a trade-off between $CO_2$ uptake and water loss. So, when water access is low, stomatal conductance needs to be reduced in order to conserve water. Naturally, this also reduces photosynthesis and thereby the amount of carbohydrates within the plant (Chapin et al., 2002).

In about 85% of vascular plant species, carbon is fixed through $C_3$ photosynthesis. This photosynthetic pathway is generally limited by the products of the light reaction (i.e. chemical energy) and by the concentration of $CO_2$ in the chloroplast. However, in many warm high-light environments, such as tropical grasslands and savannas, $C_4$ photosynthesis dominates. The advantages of $C_4$ photosynthesis in these areas is that due to an extra set of carbon-fixation reactions, more chemical energy that can be used in the carbon fixation reaction can be produced for each $CO_2$ that is fixed. Moreover, the $C_4$ photosynthetic pathway reduces the concentration of $CO_2$ within the leaf, which increases the concentration gradient between the atmosphere and the inside of the leaf. Hence, $C_4$ plants can absorb $CO_2$ with a more tightly closed stomata and thereby reduce water loss. The drawback of this metabolism is that the additional carbon that is fixed by photosynthesis occurs at the expense of a higher energy cost and is therefore only beneficial in warm, high-light environments (Chapin et al., 2002).

In the Sahel, water is only abundant for a few months during July to September – a period that accounts for about 80% of the annual precipitation (Nicholson, 2009). So, there is a need for low stomatal conductance to minimize water loss. High photosynthetic capacity, and consequently high amounts of chlorophyll, is of little use when the plant must keep the small amount of water that is available to them (Chapin et al., 2002). Hence, once the plants have fructified and secured next year's growing season, the plants in the semi-arid Sahel need to match their photosynthetic capacity to water availability and therefore reduce their chlorophyll content, which makes grasses turn yellow toward the end of the growing season. In fact, plants in low-resource environments reduce the amount of light absorbed through photosynthesis more than they reduce the efficiency of light being converted to carbohydrates

(Hiernaux et al., 2009, Chapin et al., 2002), making them able to grow for a longer time than might be expected only judging by their greenness, or amount of chlorophyll.

**Importance for keeping livestock**

Amount of vegetation is an important factor for feeding and raising livestock. Thus, understanding and monitoring the variations of herbaceous biomass is of importance for keeping livestock; maybe to a larger extent in arid areas where most part of the year is too dry to support growth of many plants (Hirata et al., 2007).

The main sustenance for livestock in the Sahel is grass, bushes and trees. The vegetation being consumed is dependent on the selectivity of different types of livestock; cattle preferably graze on grasses while sheep and goats prefer forbs (Desalew et al., 2010). The annual grasses are restricted to the rainy season as they cannot grow when there is not sufficient moisture in the top layers of the soil. In addition to annual grasses, there are also a few perennial species and bushes and trees which, as opposed to the annual grasses, have the capability of storing nutrients and tapping ground water reserves in the deeper soil layers. These species also offer feed – especially during the dry season when woody forage exerts the main source for protein and carotene (Tucker et al., 1985).

Vegetation also varies in quality according to their stage of growth and maturity. Plants are most nutritious during the early growing stages. Once mature the nutritive value of plants declines – especially for herbaceous plants (Desalew et al., 2010). At the same time the plants´ content of fibre, lignin and cellulose increase. These substances serve as protection from high temperatures and evapotranspiration. But, they also reduce their nutritional content and digestibility, making them more indigestible to animals (Powell et al., 1996). Therefore the early growing stages are important for the animals and thereby the farmers.

## 1.3 Aim

The overall aim of this study was to find a way of simplified biomass measurements on Sahelian grasslands. More specifically, the objectives were:

- Investigating whether the information in digital color photographs held information that correlated with AGB, applying greenness indices and unsupervised image classification.
- Investigating whether grass height correlated with AGB.

Moreover, the aim was to discuss whether any of these methods could replace traditional biomass measurements, and if it could serve as reference data for satellites monitoring vegetation.

## 1.4 Study Area

**The Sahel and the summer season**

The Sahel region is the transition zone south of the Sahara and north of the tropical savannas (Herrmann et al., 2005), with Senegal in the west and Sudan in the east. The region is dry for most of the year and receives almost all of its rainfall from July - October; giving a mean annual rainfall of 200-600 mm per year (Hein & De Ridder, 2006). Some factors causing this rain, and their interrelations, are debated. Broadly, however, the reason for this yearly rainy season is the northward shift of the Intertropical Convergence Zone (ITCZ) during the boreal summer (Giannini et al., 2003) and the large seasonal temperature and humidity differences between the Sahara and the equatorial Atlantic. As the maximum radiation from the sun moves north during boreal summer, the land warms faster than the ocean and creates a thermal contrast between the Sahara and the equatorial Atlantic, resulting in a low pressure zone over the Sahara and a high pressure zone over the equatorial Atlantic. As a consequence of these pressure zones moist rain-bringing air blows in from the ocean over West Africa (Cornforth, 2012). The ITCZ then shifts south again in September to October.

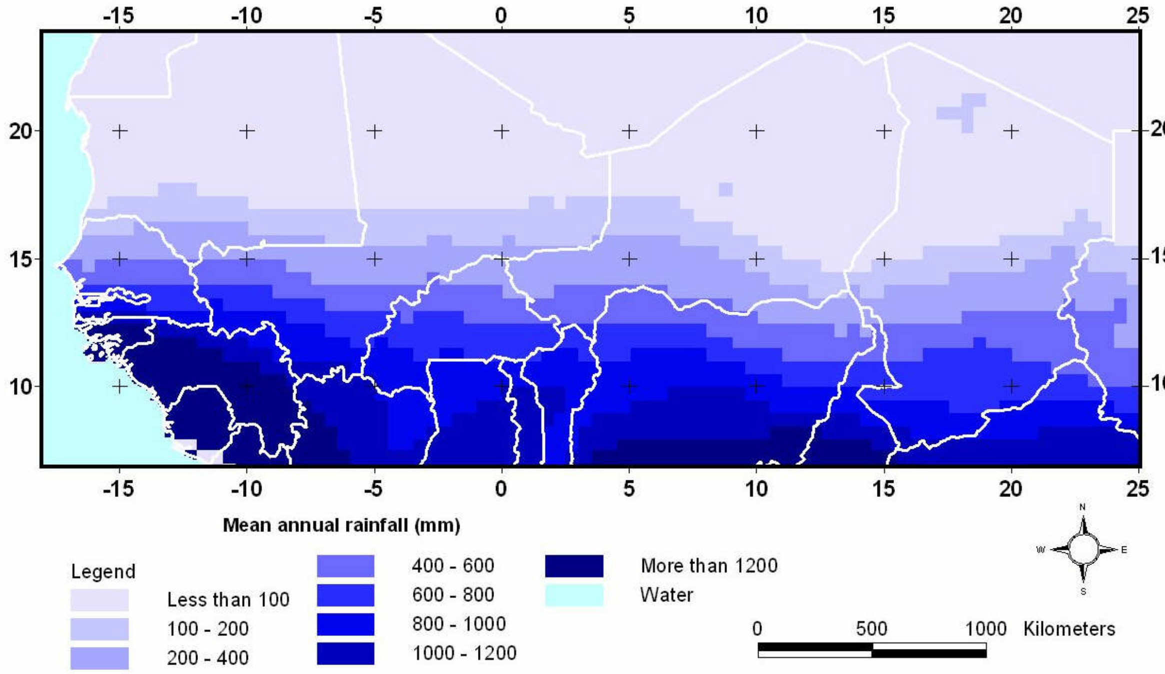


**Figure 1. Mean annual rainfall based on 2.5 degree (~ 275 km) gridded rainfall data from 1982 to 2003 (Töttrup & Helldén, 2007).**

Recent work has shown that much of the year-to-year changes in Sahel rainfall are caused by changes in sea surface temperatures (SST's) in the Gulf of Guinea, as the SST's affect the displacement of the ITCZ (Liu et al., 2012). Warmer SST's in the Gulf forces the ITCZ to shift south, from the Sahel, while cooler SST's in the Gulf cause a northward shift of the ITCZ – bringing more rain to the Sahel. This phenomenon is increased through positive land-atmosphere feedbacks (Wang & Eltahir, 2000). For instance, during dry years, there is less vegetation, which brings less evaporation from the land. Thereby precipitation is reduced even further.

**Sahel drought**

Drought is a slowly developing natural hazard, mostly caused by a decrease in rainfall over a certain period of time (Mishra & Singh, 2010). Over the past decades the Sahel region has experienced several widespread droughts, the most extensive occurring in 1973, 1984, 1990 and 2010. These droughts caused losses of livestock and naturally had a negative impact on the households' breadwinning. Since then, increased rainfall and vegetation greenness has been observed in analyses of satellite imagery (Nicholson, 2005; Huber et al., 2011; Perez et al., 2012).

Factors controlling the environmental changes in the Sahel are still debated. Some authors suggest an ongoing desertification in the area followed by vegetation decline due to anthropogenic overuse of resources (Hein, 2006; Moulin & Chiapello, 2006). Hein (2006), for instance, argues that ongoing land degradation occurs despite observed increases in vegetation greenness in the area. He stresses that the upward trend in rainfall has masked the ongoing land degradation, which in turn would imply that the Sahelian population may be more vulnerable to land degradation than what is currently assumed.

On the other hand, authors rejecting this theory state that most of the change in Sahelian vegetation greenness can be explained by precipitation changes. This is discussed e.g. in Hickler et al. (2005), where precipitation was identified as the primary driver at larger scales when studying factors controlling an ecosystem model that closely reproduced the observed greening of the Sahel. Herrmann et al. (2005) attempted to detect a possible “human signal”, which could not be found after removal of the climate signal from a Normalized Difference Vegetation Index (NDVI) data set. Lately though, Herrmann and Tappan (2013) have acknowledged the importance of additional field data in order to attain data of species composition. They conclude that despite observed greenness through satellites, this does not necessarily relate to an increase in all types of vegetation. Trees, for instance, had decreased in all of their study sites over a 27-year period – especially species that can be associated with anthropogenic pressure. For the savanna ecosystem this can be damaging, as woody vegetation to a higher extent than grass retain soil water storage and soil stability (Reid et al., 1999).

**Senegal**

Senegal is the most westerly country in Africa and has over the last 100 years experienced a substantial population increase and is currently increasing by 2,51% per year (CIA, 2013). This has resulted in increased agriculture and grazing intensities as well as larger areas occupying this type of land use, which can be seen in figure 3 (FAO Stat, 2013; Parton et al., 2004). Furthermore, trees have been removed for charcoal production and drilling of water wells, which have also resulted in increased grazing area, with a positive feedback on population growth (Valenza & Diallo, 1972 *in* Parton et al. 2004).

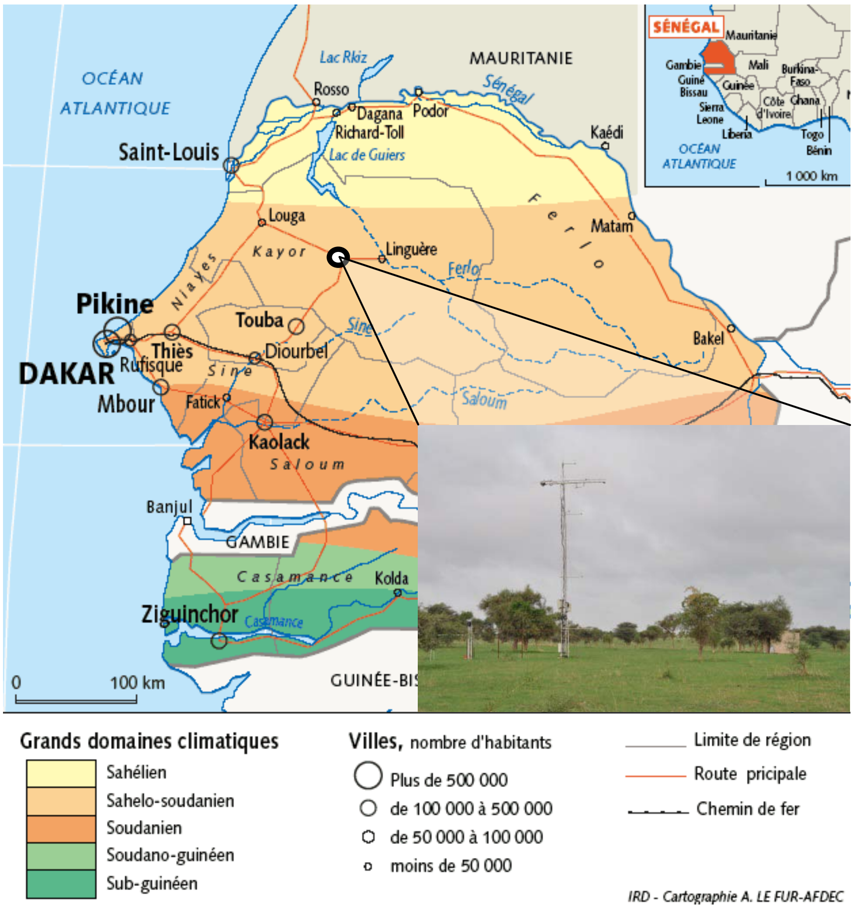


**Figure 2. Map of Senegal with climatic zones. The location of Dahra is marked out with a point in in the northern part of the Sahelo-Sudanian zone (modified from Au Senegal, 2012).**

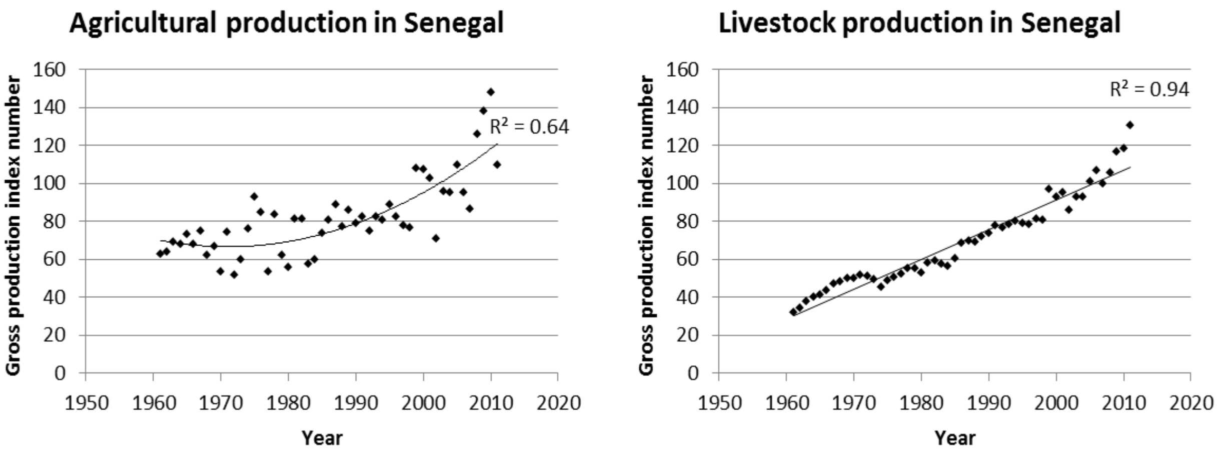


**Figure 3. Agricultural and livestock production in Senegal. To obtain the index, the aggregate for a given year is divided by the average aggregate for the base period 2004-2006 (index no 100). Data from FAO Stat (2013).**

**Dahra**

In Dahra, which is the location of the study site, grazing is the dominant land use. Sheep, goats, cows and dromedaries graze on this land, which is dominated by open grasslands with fine-leaved annual grasses such as *Schoenefeldia gracilis, Dactylotenium aegypticum, Aristida mutabilis and Cenchrus bifloures*, but some perennial grasses can also be found (Fensholt et al., 2006). Sparse vegetation consisting of thorny shrubs and trees (*Balanites aegyptiaca* and *Boscia senegalesis*) (Diallo et al., 1991) are also interspersed between the grasses and herbs. Shrubs and Acacias last throughout the year while grasses start growing at the onset of the rainy season in late July and last until some weeks after the end of the rainy season. These grasses make up the main sustenance for grazing animals in the area and are therefore important to monitor, as the livestock is a vital part of the Senegalese peoples' breadwinning (Tucker et al., 1985).

Climatic research has been carried out in Dahra for about a decade (Fensholt et al., 2006). Nowadays sensors measuring e.g. precipitation, soil moisture, wind speed and atmospheric carbon are situated at the study site and these masts are also one of the main reasons this biomass study has been carried out at this very location. Figure 4 shows a view of the Dahra test site and figure 5 shows temperature and precipitation from March to November 2011. Hence, the rainy season covers the time span of the performed field work.

Figure 4. Photograph from the Dahra test site in July.

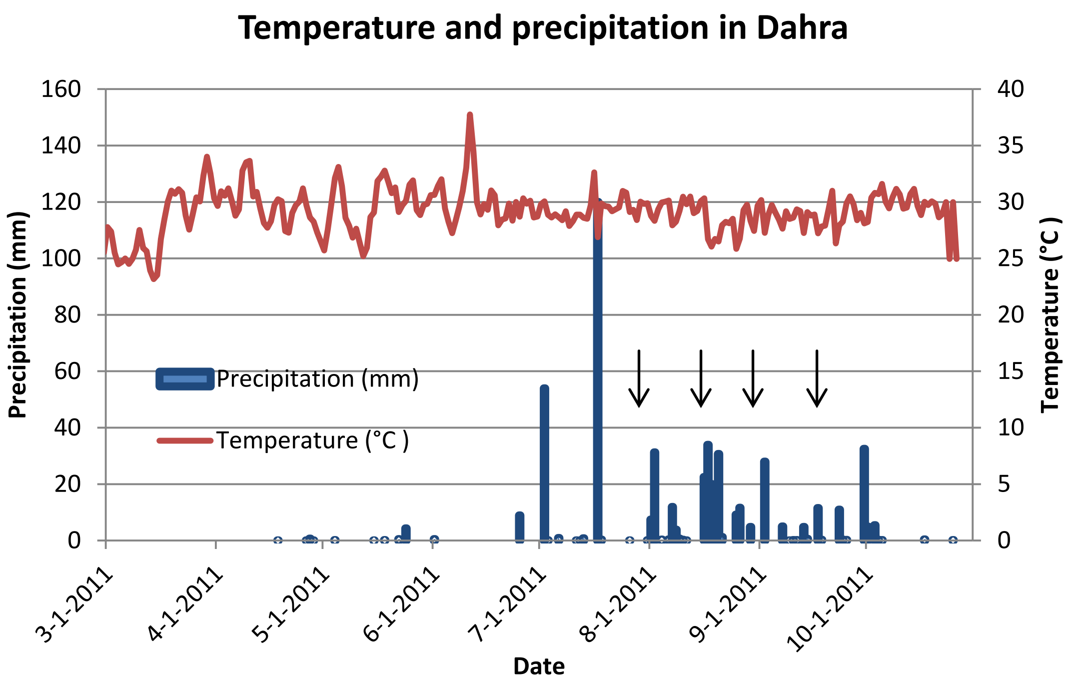


**Figure 5. Daily mean temperature and daily precipitation at the Dahra test site, 26/2/2011 to 26/10/2011. The smallest precipitation bars represent 0.1 mm. Black arrows indicate biomass measurement occasions. Courtesy of Fensholt, University of Copenhagen.**

# 2. Theory

## 2.1 Spectral properties

The camera records emitted electromagnetic energy, i.e. *radiance,* from a certain object. The radiance is an indicator of how bright an object that is received by an optical system will appear. Spectral radiance expresses radiance as a function of wavelength, so an object that appears blue has relatively high radiance (i.e. is bright) at blue wavelengths, at least compared to the radiance in green and red wavelengths. Radiance depends on the amount of incoming light; more incoming light inevitably leads to more light being reflected and recorded by a certain sensor (Lillesand et al., 2008). The DCI's used in this study register visible light (400 – 700 nm) that is reflected from a certain object, here grasslands.

Ecological studies based on or aided by data derived from satellite images differ from DCI's in that they do not only take the light that is reflected from an object into account, but also incoming light. By measuring the percentage of incident energy that is reflected, objects within the covered area do not depend on incoming light and can thereby more feasibly be studied relative to each other, based on differences in their *spectral reflectance*:

$$\text{Spectral reflectance [\%]} = \frac{\text{energy of wavelength } \lambda \text{ reflected from the object}}{\text{energy of wavelength } \lambda \text{ incident upon the object}} * 100$$

The proportion of energy reflected, absorbed and transmitted varies for different features. Moreover, there is a wavelength dependency which means that even within a certain feature type; reflection, absorption and transmission vary at different wavelengths. An example of a spectral reflectance curve, generated by an objects' spectral reflectance as a function of wavelength can be seen in figure 6, which shows that green grass has a clear peak at green wavelengths (500 – 600 nm) while sands have a higher reflection than grass all over the visible part of the reflectance spectrum, most notably in the green and red wavelengths (600 – 700 nm).

The spectral reflectance characteristics of plants are defined by their biochemical composition and physical properties, e.g. cell structure and lignin content. In addition, the plants' spectral characteristics are influenced by factors such as spectral properties of the source (here; the sun), viewing angle, leaf surface structure, moisture conditions and soil type (Myneni & Asrar, 1994).

In plants, reflectance is related to the spectral absorption (Zwiggelaar, 1998) by pigments and water. The most important pigments (and absorption bands) are: chlorophyll a (435, 670-680, 740 nm), chlorophyll b (480, 650 nm), α-carotenoid (420, 440, 470 nm), β-carotenoid (425, 450, 480 nm) and water (970, 1450, 1944 nm). Most plants contain a combination of these pigments and water, thus leading to an absorption spectrum that does not always have sharply defined peaks. Absorption is relatively large in the red and blue bands due to pigments (mainly chlorophyll). Whereas lower absorption (thus higher reflectance) occurs in the green band than in the red and blue ones. Apart from the water absorption peaks, reflectance in near infrared (NIR) is very high in leaves due to cell structure. Plants use visible light in photosynthesis, but are vulnerable to NIR wavelengths, which may damage them (Zwiggelaar, 1998). Because of low absorption in NIR, with a subsequently high reflection in this part of the spectrum, green vegetation is easily distinguished when vegetation is studied in these longer wavelengths. So, the NIR part of the spectrum provides a lot of important information. However, cameras able to handle NIR wavelengths are generally expensive (Zwiggelaar, 1998) and are, as already mentioned, not covered in this study.

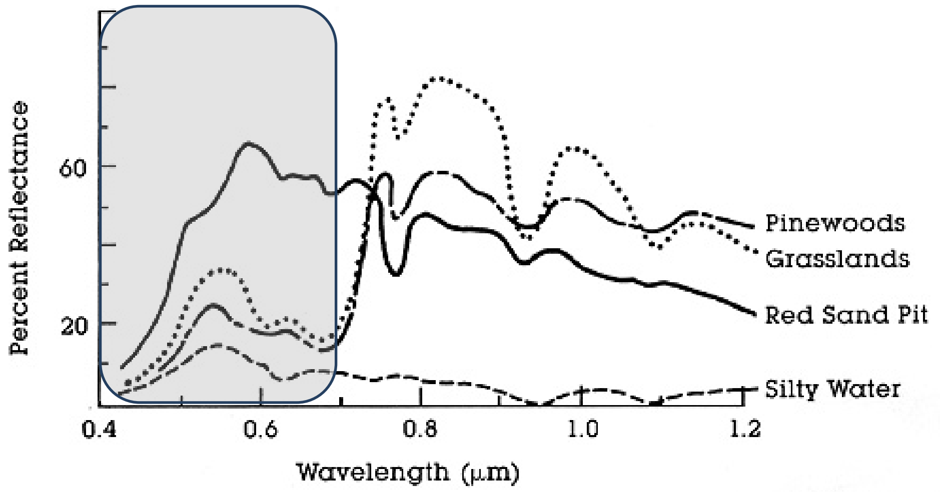


**Figure 6. Spectral reflectance curve for some land cover categories. The visible part of the reflectance curve lies within the grey zone. Grasslands and red sand pit are of most interest for this study (modified from NASA, 2011).**

In arid and semi-arid areas, challenges are faced when estimating AGB through spectral indices due to soil-vegetation spectral mixing (Ren et al., 2011). That is; in sparse canopy situations, indices attempting to describe properties of vegetation tend to be affected by a significant contribution of soil reflectance (Boschetti et al., 2007).

Asner (1998) investigated the relative contribution of leaf, stem and litter optical properties to vegetation reflectance data in four different biomes using a spectroradiomater. For grasslands, they found that standing litter and LAI were the dominant controls on canopy reflectance, where litter, which showed a high reflectance in the visible range of the spectrum, played a more important role here and LAI in the NIR range of the spectrum (figure 7).

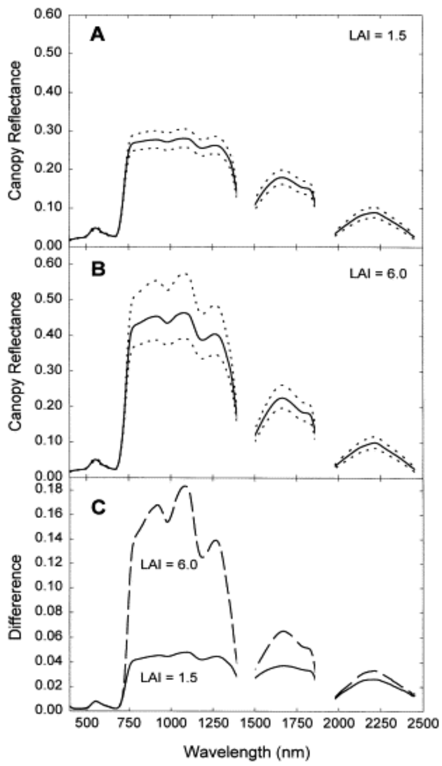


**Figure 7. Effects of canopy reflectance simulated for two LAI scenarios. Strong atmospheric absorption near 1400 nm and 1900 nm due to water vapor prevented measurements and modeling of these regions. LAI=1.5 is typical for grasslands (Asner 1998).**

## 2.2 Previous vegetation studies using digital camera images (DCI's)

Spectral vegetation indices are widely used for monitoring, analyzing and mapping temporal and spatial variations in vegetation structure and biophysical parameters (Gitelson et al., 2002). Most vegetation indices combine information included in the red and NIR spectral bands. However, the efficiency of the indices are generally limited due to difficulties in separating moderate and high chlorophyll contents, as the reflectance in NIR often levels off with an increase in vegetation fraction (VF). Reflectance in the visible range is less species specific than in the NIR, as it is mainly affected by pigment content and composition and to a lesser extent by factors such as canopy architecture, cell structure and leaf inclination. However, when the purpose of a study does not depend on classifying single species there is an advantage in using color indices as they accentuate a particular color (e.g. greenness) and should be intuitive for the human eye (Gitelson et al., 2002).
The use of digital camera images (DCI's) in vegetation studies is not new. As information on these sorts of studies has not been found for the Sahel, indices found in studies conducted in other regions have been applied to this project.

Richardson et al. (2007), Crimmins and Crimmins (2008), Gitelson (2002) and Westergaard-Nielsen (2010) have all used the digital numbers (DN's) of DCI's for detection of vegetation and correlated this versus parameters such as VF, phenological events or green-up after snow cover. Some different algorithms have been applied. Common for all is that they attempt to create and use greenness indices; algorithms that enhance the green band in the images in order to better detect green vegetation. They also make up the base for the algorithms described in section 3.2.

Richardson et al. (2007) evaluated the green-up signal extracted from DCI's against changes in VF to monitor spring green-up in a deciduous northern hardwood forest. They compared their green-up signal to changes in in situ broadband NDVI, the photosynthetically active radiation absorbed by the canopy ($f_{APAR}$) and the theoretical light-saturated rate of canopy photosynthesis ($A_{max}$). The origin of their index (Eq 1) is based on their findings of the canopy having a stable green signal throughout the season, but declining red and blue signals. Hence, the canopy became relatively greener. They also found that the blue channel responded well with green-up but was found to be more sensitive to incident radiation than the other two. They concluded that DCI's from webcams offer an inexpensive way of quantifying phenological changes and suggest that a larger amount of cameras could be used in a regional or national phenology monitoring program.

Crimmins & Crimmins (2008) observed aerial plant cover and flower blooms using digital repeat photography and concluded that together with site-specific meteorological measurements, they could enhance the understanding of environmental triggers (such as freezing) of phenologic events. They used the same index as Richardson et al. (2007) but they did not measure incoming light for comparison. However, when examining the performance of the greenness index, they compared their results using one set of only full-sun photos and one set of only full-shade photos. It was found that full-sun photos yielded relatively high brightness values in the green and red channels, while blue brightness values were relatively low. Full-shade photos, on the other hand, resulted in relatively high blue brightness values, while green and red brightness values relatively were much lower. The latter case gave lower greenness index values and a high amount of noise in the greenness signal, why they only included photos that were as free from cloud shadows as possible in their study (Crimmins & Crimmins, 2008). The reason for these findings is probably that the total reflected energy is reduced within a shadow, and the spectral response is shifted towards shorter wavelengths – a phenomenon caused by Rayleigh scattering, which appears when radiation interacts with atmospheric molecules and particles that have a smaller diameter than the wavelength of the interacting radiation. This primarily affects shorter wavelengths (Lillesand et al., 2008). Hence, the shadowed images appear darker and bluer than the full-sun images.

Richardson et al. (2007) and Crimmins & Crimmins (2008) used the same algorithm for their index:
Eq 1: $GV_R = (green - red) + (green - blue)$

Westergaard-Nielsen (2010) created a Normalized Difference Greenness Index (NDGI) for $CO_2$-flux, vegetation greenness, snow cover and snow distribution from DCI's. This index was considered less sensitive to brightness than some of the previously mentioned studies (e.g. Richardson, 2007 and Crimmins & Crimmins, 2008). Westergaard-Nielsen's study was performed in the high-arctic parts of Greenland using images from two locations, where photos had been taken mid-day each day from 1997 (in the Zackenberg valley) and 2007 (in Kobbefjord) until 2010 (both locations). The NDGI was found to correlate with ground truth measurements of spring green-up, snow depth and $CO_2$ flux.

Index from Westergaard-Nielsen (2010):
Eq 2: $GV_{W\text{-}G} = \frac{((2*\text{green})-(\text{red}+\text{blue}))}{((2*\text{green})+(\text{red}+\text{blue}))}$

Gitelson et al. (2002) studied reflectance of wheat canopies in both the visible and the NIR ranges of the spectrum, looking at digital photographs taken in field, reflectance spectra in field and satellite derived data from the National Aeronautics and Space Administration's (NASA's) Moderate Resolution Imaging Spectroradiometer (MODIS) and the European Space Agency's (ESA's) Medium Resolution Imaging Specrometer (MERIS). Ultimately, they attained VF through digital photographs and tested two indices using only the visible part of the spectrum (one using only green and red and one that also included blue). They visually analyzed their results and concluded that there was no misclassification of dead vegetation as green material and shadowed soil was correctly classified as soil. They also compared satellite data that had been analyzed in the same manner as their DCI's to (1) the VF attained through DCI's and (2) NDVI and green NDVI (including NIR) from satellites. They found that the index using red, green and blue correlated best with VF and propose the reason for this would be that for wheat canopies, green and red are most sensitive to VF, while a subtraction of blue would correlate for atmospheric effects in red and green. Moreover, NIR leveled off or even decreased at or near midseason and therefore inclusion of NIR was considered a limiting factor when estimating VF.

Index from Gitelson (2002):
Eq 3: $GV_G = (\frac{green-red}{green+red-blue})$

## 2.3 Color mixing

In digital color images there are three color bands, registering brightness values, or digital numbers (DN's) for the red, green and blue part of the spectrum, respectively. The bands attain DN's between 0 and 255. So a pixel that is purely red has the DN's: 255-0-0 (R-G-B), a green pixel has the DN's: 0-255-0 and a blue one 0-0-255. All colors that are not purely red, green or blue are mixtures of these. Hence, a pixel that is yellow attains the DN's 255-255-0, since yellow is a mixture of red and green, as can be seen in figure 8. In order to link this to the images from the test site one could say that the images covering large amounts of green grass have many pixels with a high value in the green band whilst images covering yellowing grasses have high pixel values both in the green and in the red band.

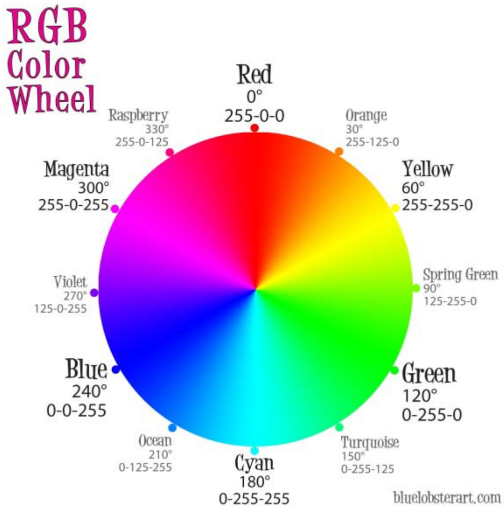

**Figure 8. RGB color wheel showing the three base colors red, green and blue and their mixing colors (Blue Lobster art and design, 2013).**

Images covering more bare soil than vegetation are likely to have more pixels with high values in green and red based on the spectral properties of sand (figure 6).

## 2.4 Leaf Area Index (LAI)

Long-term monitoring of LAI; the ratio of leaf area per unit ground surface area is used as a parameter for calculating surface photosynthesis, evapotranspiration and productivity. LAI accounts for much of the biome differences in carbon gain during the growing season and an increase in LAI relates directly to an increase in biomass (Chapin et al., 2002; Edrisinghe, 2011).

A number of LAI satellite products have been developed for optical remote sensing of vegetation. They are aimed at retrieving the spectral characteristics of leaves, which are determined by the internal biochemical structure and chlorophyll content (see section 2.1). However, they are not always fully reliable as they reach saturation when cloud or vegetation cover is dense. Furthermore, they differ slightly as they use different algorithms for estimating LAI (Gessner et al., 2013). Gessner et al. (2013) concludes that the MODIS LAI product (EROS, 2012) which is used in this thesis performs well with respect to spatio-temporal resolution and occurence of data gaps when covering West Africa as long as clear-sky conditions occur, but also discuss that it seems to be particularly sensitive to cloud contamination when compared to other freely available LAI products.

## 3. Methods

### 3.1 Biomass measurements in the field

Biomass measurements were performed at four separate occasions during the growing season in 2011 (July 29 - August 1, August 12 – August 15, August 28 – September 1, September 17 – September 19). The first one at the onset of the growing season and the last occasion took place at the peak of the growing season.

Biomass measurements are performed at the Dahra test site each year during the growing season. This is done on 28 different sampling points forming a cross according to the sampling scheme in figure 9. The aim was to perform all biomass measurements in exactly the same way as the measurements are generally performed, but a communicative error of the sampling procedure resulted in some inconsistencies during the first sampling occasion (July 29 – August 1), leading to roots being collected as well as the AGB. The root weight was included in the analyses and this will be brought up in the discussion, but the roots being a very small part of the grass straw they will be treated the same way as the biomass from the latter three measurement occasions.

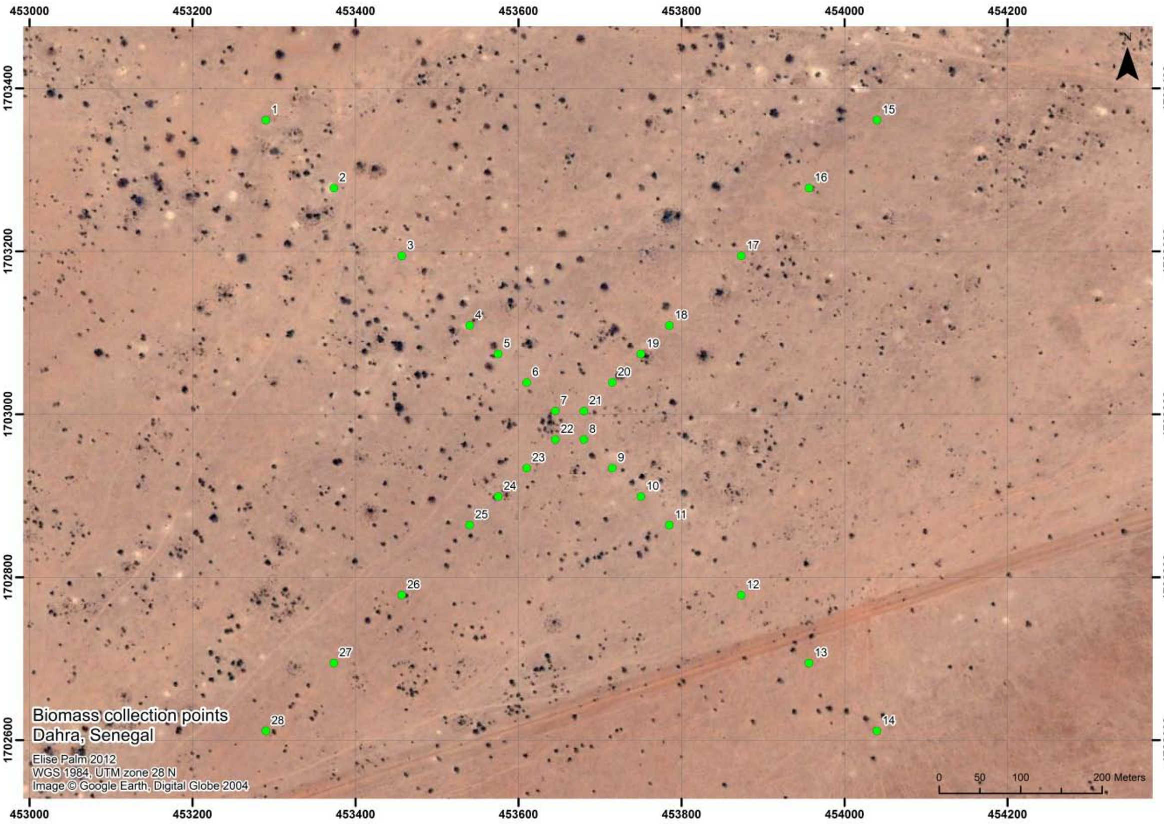


**Figure 9. Quickbird (Digital Globe, 2011) image with sample points for the Dahra test site. All biomass measurements started off at the NW corner and followed the point order up to point 28 (region: UTM, zone 28 N).**

### Collection of "ground-truth" data

In the field, a steel frame $1m^2$ in size was laid out on the sampling point (figure 10). Firstly, grass height was measured using a scale. Then AGB within the frame was cut with scissors. The biomass was collected in cotton bags and was after collection hung outdoors until it was dry enough to be stored in attendance for further drying in oven. Oven-drying of biomass was done for three consecutive days in $40^{o}C$. If still not sufficiently dry, the procedure was repeated once more. Finally, each bag was separately weighted on a balance with a resolution of 1g.

**Figure 10. Grass cut off within the 1 $m^2$ frame on sample occasion 3. At the lower left edge grass lacking since the previous sampling occasion is visible.**

At each sampling occasion the quadrat was moved northward, edging the quadrat of the preceding sampling occasion. So the exact GPS-point was only used at the first measurement occasion. Figure 11 shows images from point 19 and illustrates an example of the ground at the four different dates of sampling. Naturally, the vegetative differences were not exactly similar for each point. At some points vegetation grew slightly faster and at other points slightly slower. However, point 19 was chosen as it was considered to be representative and lies close to the center of the site, but still not too close to the meteorological measurement equipment.

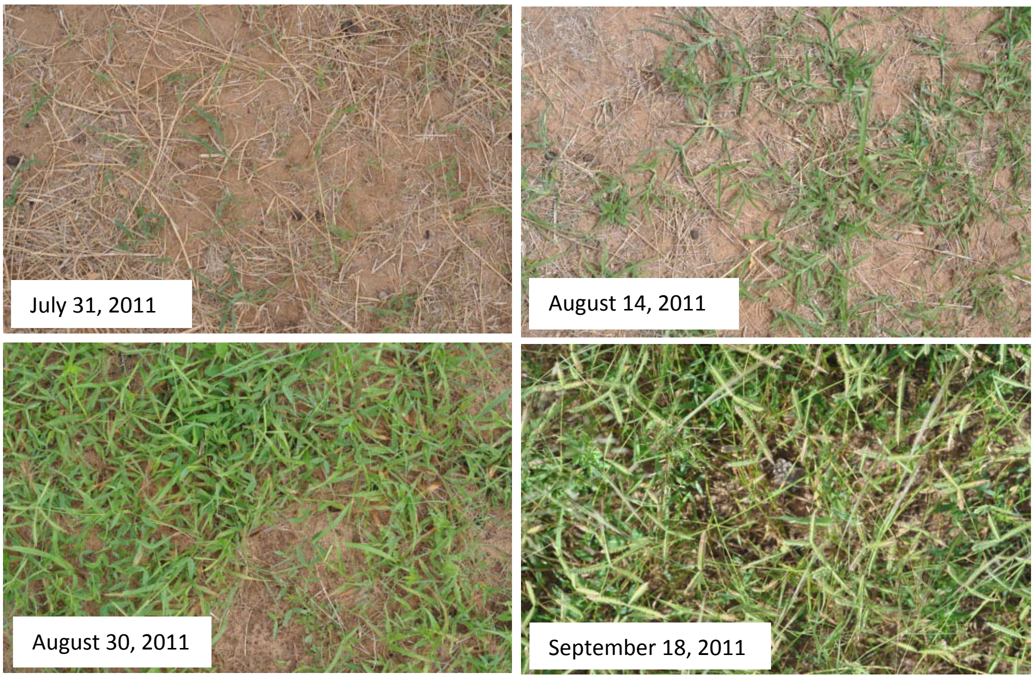


**Figure 11. Example of images taken at each sampling occasion. From point 19.**

**Photographing the plots**

Before biomass was collected on a plot, a digital photograph was taken. The camera used was a Nikon D90 camera with a Nikon AF Nikkor lens, 50 mm focal length. Shutter speed was set to a constant 1/250 sec in order to avoid blurry images due to grass moving in the wind while f-stop was allowed to change with changing light conditions. Each photograph was taken vertically at a distance of 1.20 m. Six images of ground completely free from biomass are also included in the analyses. These are taken at the site but not at any of the measurement points.

## 3.2 Data analysis

Advantages of using DCI's are, in addition to the reduction in labor demand, that they are cheap and offer three spectral bands: red (R), green (G) and blue (B). For monitoring purposes this offers objective methods for studying the bands through digital image analysis, as opposed to e.g. older analog images. All analyses were performed using JPEG (Joint Photographic Experts Group) images; these are compressed images where neighboring pixels of almost the same color are joined. This compression could potentially affect the analyses but Lebourgeois et al. (2008) reject this effect in a vegetation study using DCI's.

### 3.2.1 Separate bands

All JPEG images were separated into R, G and B. For each image the mean R, G and B value was calculated. So; resulting DN values are averages of the brightness in the images that were collected at the point for biomass measurement. These results were visualized in scatter plots to describe spectral changes over the vegetation season.

### 3.2.2 Greenness values

The following algorithms have been applied in this project and will from now on be referred to as greenness values (GV's):

Richardson et al. (2007) and Crimmins & Crimmins (2008) used the same algorithm:

Eq 1: $GV_R = (green - red) + (green - blue)$

Westergaard-Nielsen (2010):

Eq 2: $GV_{W\text{-}G} = \frac{((2*\mathrm{green})-(\mathrm{red}+\mathrm{blue}))}{((2*\mathrm{green})+(\mathrm{red}+\mathrm{blue}))}$

Gitelson (2002):

Eq 3: $GV_G = (\frac{green-red}{green+red-blue})$

As the JPEG images were already separated into R, G and B, GV for each separate pixel was calculated and then averaged over the whole image. The final GV's were then further analyzed and compared with biomass. First, a scatterplot was produced in order to visually examine the basic shape of the relationship. Then a correlation analysis was conducted. The resulting correlation coefficient from this test was tested for statistical significance (p-value) through a t-test in GraphPad Software (2005) to investigate whether the correlation coefficient between biomass and each of the indices showed a significant correlation, thus rejecting the zero hypothesis stating that no relationship between x and y (i.e. image/GV's and biomass) occurs.

### 3.2.3 Unsupervised classification

In addition to using above algorithms, a collection of images were randomly selected to be processed using unsupervised classification in IDRISI Andes (Clark Labs, 2006). There, the algorithm Iterative Self-Organizing Data Analysis Techniques $A^2$ (ISODATA) was used. This

classification method orders the data in the wavelength bands into clusters based on the spectral groups present in the data set. Firstly, one decides on the number of clusters the data should be ordered into. Then each pixel is assigned to the cluster whose mean vector is closest. This assignment is done throughout the classification of each pixel, so from one iteration to the next, clusters are merged, split and deleted. Thereby the clusters change throughout the classification process until all pixels have been classified and the final classes are acquired (Lillesand et al., 2008). In this case, two spectral groups were used with the objective to automatically separate vegetation from ground by their spectral differences.
Figure 12 shows an example where three channels are grouped into two clusters. Translated into bands, the different axes correspond to R, G and B.

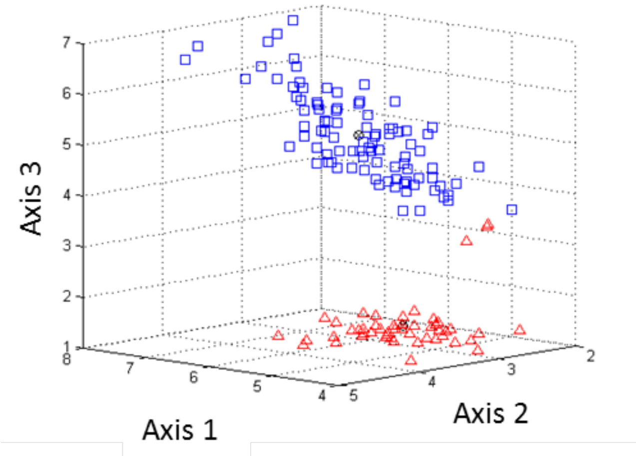


**Figure 12. Example of data ordered into clusters based on the value of each data point. For the unsupervised image classification the axes would respond to r, g and b (modified from Mathworks, 2013).**

### 3.2.4 Grass height

Just as for the GV’s, a scatter plot between biomass and grass height was produced. This was followed by a correlation test and a test for statistical significance for the correlation coefficient between biomass and grass height.

### 3.2.5 LAI

In order to correlate the results from the biomass estimations with data derived from satellites, the change in MODIS LAI (MOD15A2 from EROS, 2012) over the season was studied.

The MODIS data for LAI used here is a 1 km spatial resolution, 8-day composite. It was obtained through the online Data Pool at the NASA Land Processes Distributed Active Archive Center (LP DAAC), USGS/Earth Resources Observation and Science (EROS) Center, Sioux Falls, South Dakota (EROS, 2012).

# 4. Results

## 4.1 Separate bands

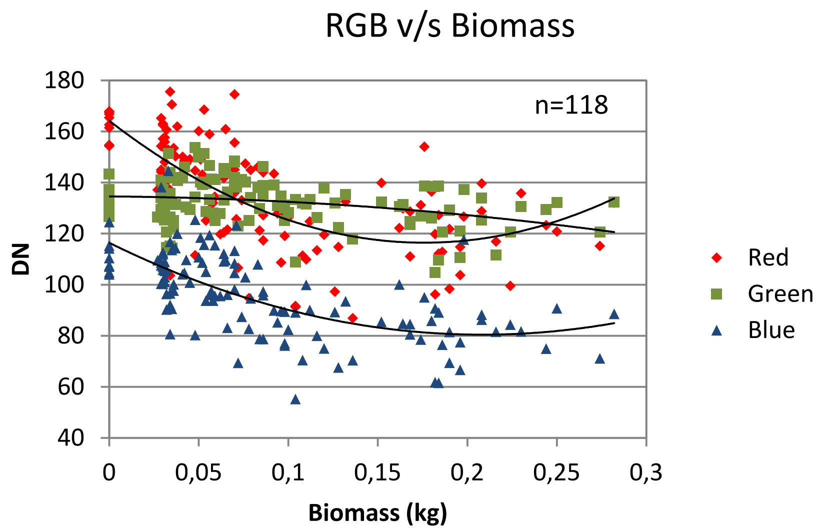


**Figure 13. Biomass v/s DN for separate bands.**

DN-values are highest for the lowest biomass weights in all bands. For the red band there is a low at biomass values of 0.15 to 0.20 kg, the values then increase, although not to the extent that can be seen for low weights. In the green band, DN declines as biomass increases. However, the decline does not commence until after biomass has reached 0.1 kg, and the decrease is rather plane. The blue band shows a similar pattern as the red one, it first declines, and increases again at higher biomass values (figure 13). Note though, that in the data set low biomass values are more represented than higher ones and therefore exert a higher influence on the curves than do higher values.

## 4.2 Greenness values

The green enhancement techniques all showed positive correlations up to the point where biomass equals about 0.15 kg (figure 14). Coefficients of determination ($R^2$) for polynomial curves for these were 0.57 for the Richardson technique and 0.56 for the Westergaard-Nielsen techniques and 0.43 for the Gitelson technique. As the negative correlation at higher biomass values indicated that the correlation between GV's and biomass collected at the fourth occasion differed from the rest of the data set, correlation for only the first three occasions was also tested separately. In these, the curve did fit the points better, and also here the Richardson and Westergaard-Nielsen techniques show a higher correlation ($R^2$=0.63 and 0.61, respectively) with biomass than does the Gitelson technique ($R^2$=0.51). Again, low biomass values are more numerous than the higher ones and affect the fit of the curves to a higher extent.

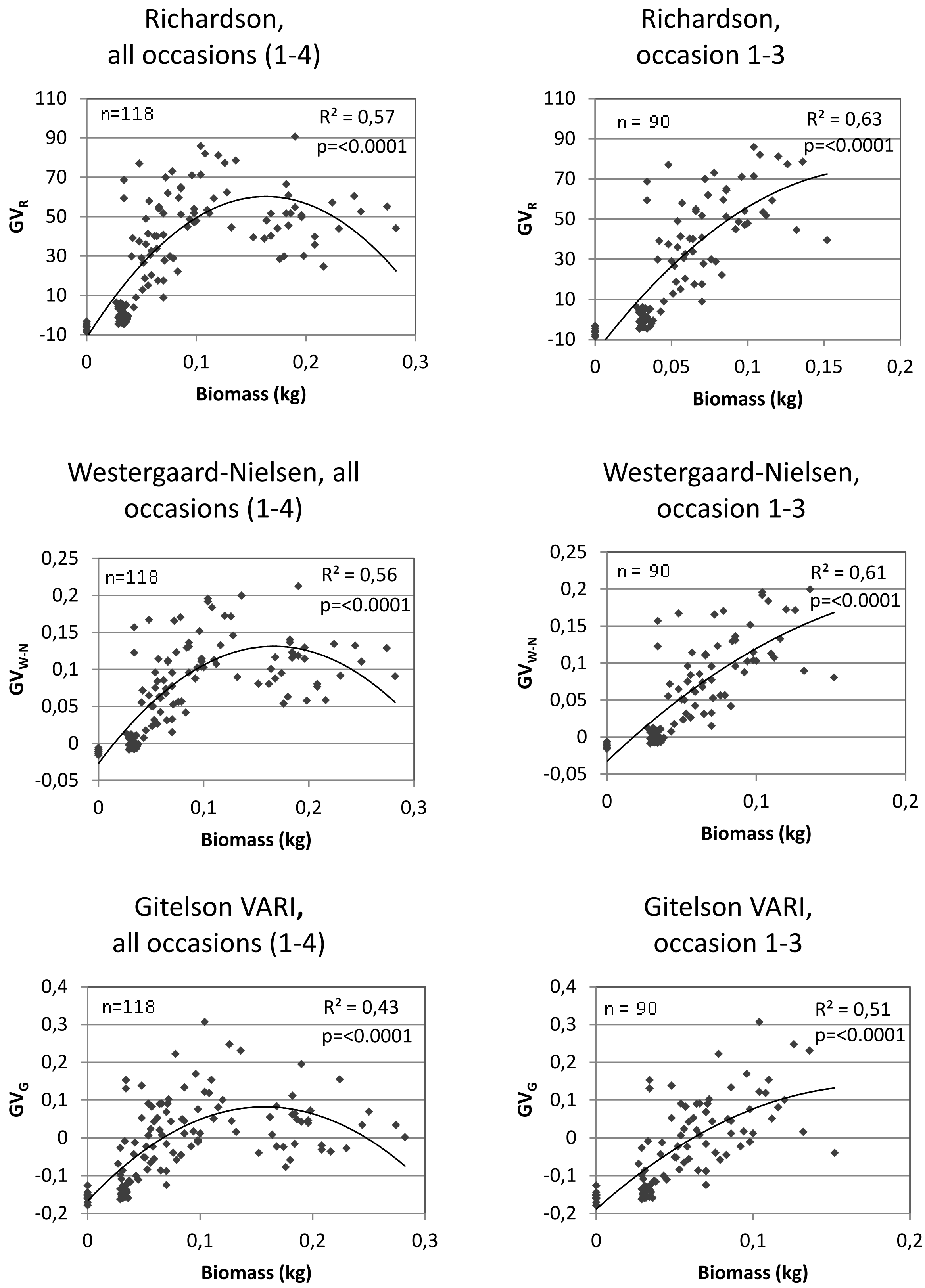


**Figure 14. Results for the different GV's. All trend lines are 2:nd degree polynomials and all correlation coefficients are significant (p=< 0.0001).**

## 4.3 Unsupervised classification

The unsupervised classification turned out to be very time consuming and laborious and was therefore first tried out on a smaller sample of images to see whether the method was likely to reveal other insights than the approach using GV's. After examining the images green grass seemed to fall into one group. However, old yellow grass could fall into either the grass group or into the ground group, and bare ground could even fall into separate groups in the very same image. So, from this, the unsupervised classification seemed to show the same difficulties as the GV techniques and was therefore not investigated further. Figure 15 points out areas where the classification is clearly not consistent in classifying soil from green grass, sometimes soil seemingly falls into the soil group and sometimes into the grass group (see circles in figure 15). All images are from sampling point 21, situated in the middle of the site.

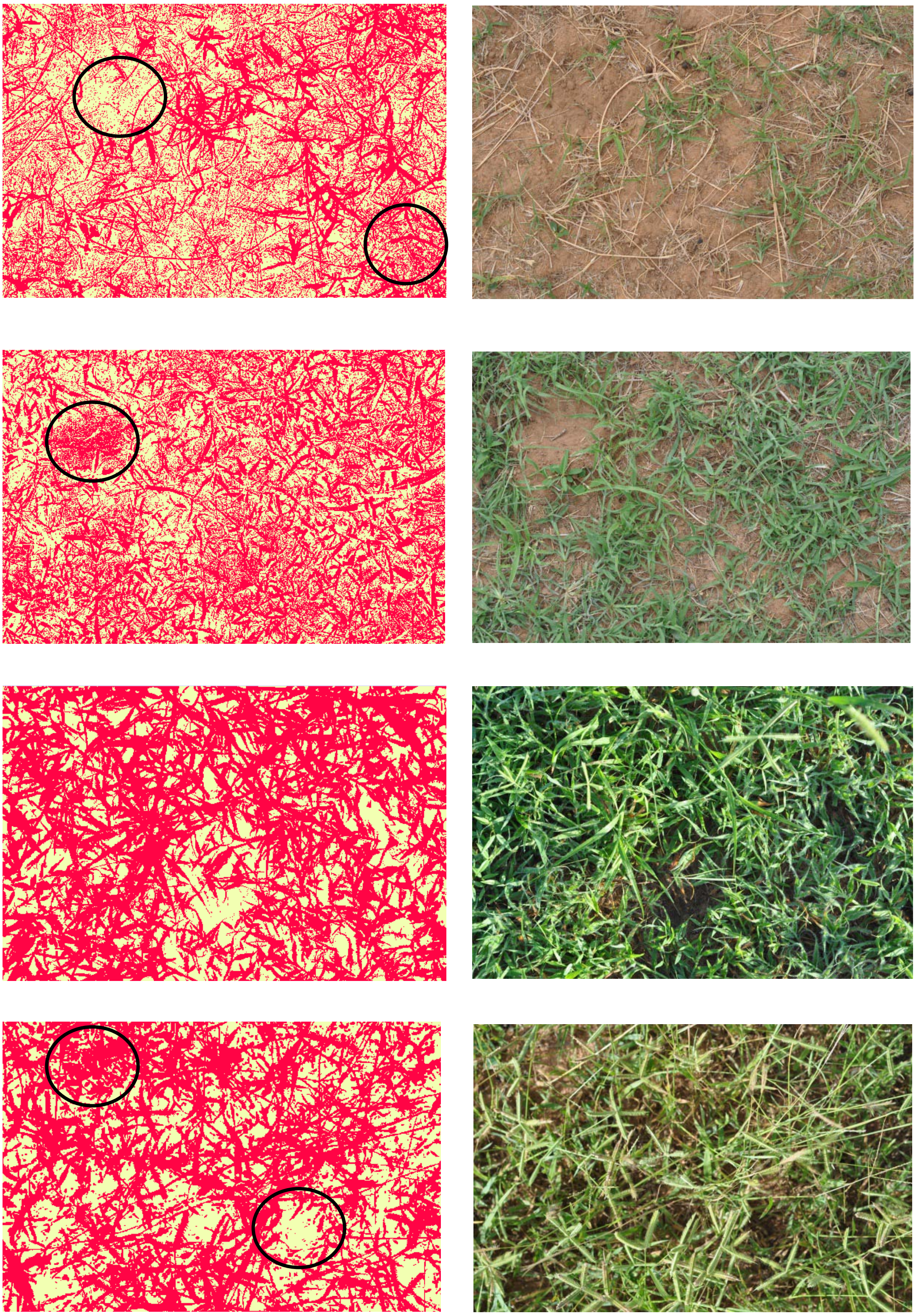

**Figure 15. Images attained through unsupervised classification of all three bands and divided into two classes (to the left). Circles point out areas that contain larger areas of bare ground but where the unsupervised classification has failed to be consistent in classifying this trait.**

## 4.4 Grass heights

The highest correlation with dry biomass was not found for any of the different GV's but for grass height, where the regression line attained an $R^2$-value of 0.79 (figure 16). Occasion 1-3 attained an $R^2$-value of 0.70 (p=<0. 0001) for linear regression.

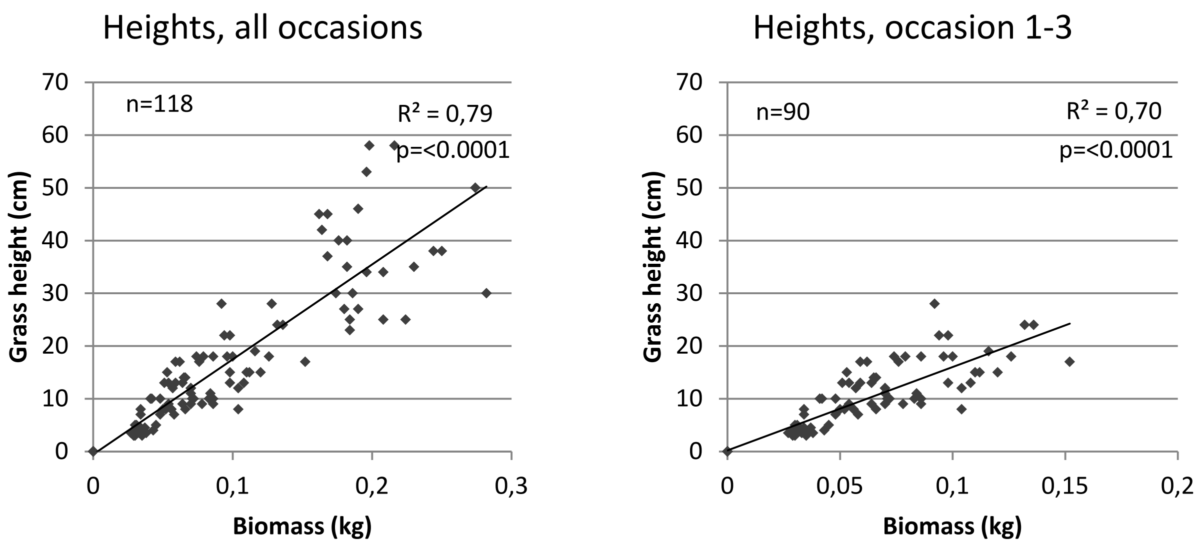


**Figure 16. Correlation between grass height and biomass. Both measured at the actual sampling point.**

## 4.5 LAI

MODIS LAI peaks around Day of Year (DOY) 250 and then dips. As is the case with GV's, it does not follow the increase in biomass at the end of the growing season. This differs from grass height, which just like biomass increases over the season (figure 17).

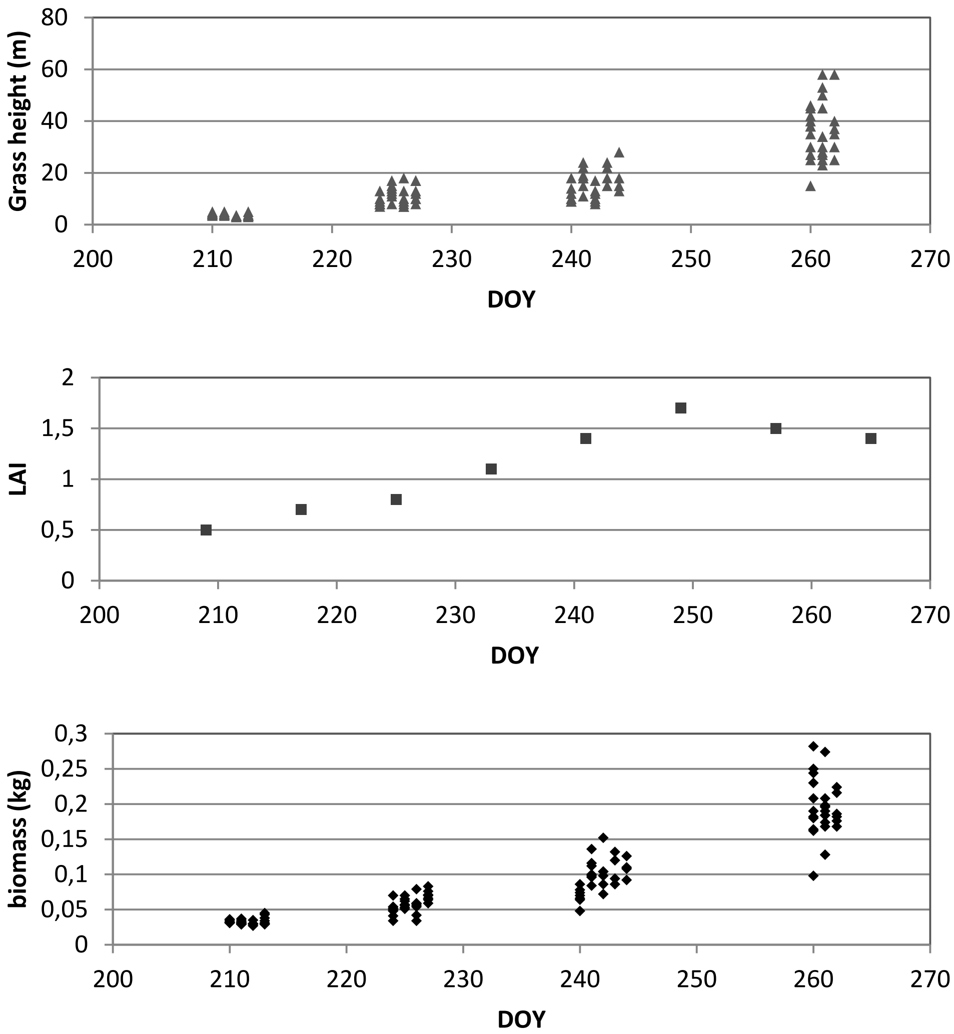


**Figure 17. Grass height, satellite derived LAI and AGB plotted against DOY during the growing season in 2011. LAI shows the same tendency for saturation as the GV's do.**

# 5. Discussion

The aim of this project was to see whether a simpler technique for biomass estimation than the traditional one could be found. DCI's were proven not to give a very reliable result. However, biomass and grass height correlate rather well. Measuring grass height is indeed a simple and quick way of acquiring an estimate and can easily be performed by the local farmers themselves.

It cannot be disregarded that the inclusion of roots during the first sampling occasion has affected the results in this thesis. However, they made out a minor part of the biomass collected and although this may have skewed the results, it is believed that the conclusions drawn from this study remain the same as if this error had not occurred.

## 5.1 Separate bands

Among the separate bands, the green one changes the least over the season while the red and blue bands decline up to the point where grasses start to dry. This follows the discussion by Richardson et al. (2007), where it is concluded that despite the fact that to the human eye the vegetation may seem greener as the growing season progresses, it is only a question of relative greenness due to lower signals in red and blue. The reason for this should be that at the onset of the growing season, there is less vegetation, or chlorophyll, to reflect green light and to absorb red and blue light. Moreover, the sand reflects highly in red and green, so the decline in red DN's is probably not solely because of chlorophyll absorption but also due to less bare ground being visible as the vegetation grows.

The green DNs do not change much over the growing season. This could possibly be explained by vegetation balancing soil in this regard; as the amount of pixels showing green-reflecting vegetation increases, pixels showing soil background decreases. Therefore, it is possible that they more or less level each other out.

## 5.2 Greenness values

The Richardson and Westergaard-Nielsen GV's did show the best fit of the trend lines to the data points ($p=<0.0001$). Both of these studies compared the indices that they developed to already recognized vegetation indices (section 2.1). Gitelson et al.'s study was conducted on vegetation (i.e. wheat canopies) that most likely has a closer resemblance to Sahelian grasslands than the northern deciduous forest and arctic tundra that were investigated in Richardson's and Westergaard-Nielsen's studies, respectively. However, Gitelson et al. (2002) visually interpreted the results of their index and concluded that it performed well. Hence, the objectiveness of that method should perhaps be questioned and lack of appropriate "truth" data when developing their index could be the reason that it does not perform better.

Richardson, Westergaard-Nielsen and Gitelson et al. did not develop their indices in order to study AGB but rather VF, i.e. the percentage of vegetation occupying the ground area in vertical projection (Liang et al., 2008), and phenology. Hence, none of these studies were actually concentrated on biomass. In section 1.2, the characteristics of plants gaining biomass after peak photosynthesis is brought up and this fact is essential for the findings in this study.
As this study for Sahelian grasslands shows that grass height correlates well with biomass, an index that is developed ideally for greenness in vertical projection is not sufficient for this purpose. At the beginning of the Sahelian growing season, grasses do spread out horizontally but as the season progresses, grasses seem to grow higher rather than spread out closer to the ground.

As yellow colors are a mixture of red and green they probably have more pixels that attain high values within the red band as well as in the green one. Since bare soil has high pixel values in the red band, green grasses have high values in the green band and yellow grasses have high values in both bands, all formulas trying to enhance either of the bands have contradicting effects on yellow grasses; meaning that the highest biomass values lie in a zone that, at least with regards to DN, is difficult to position.

Methods also using NIR are better at distinguishing vegetation from bare soil and excluding shadowing (e.g. Zwiggelaar, 1998). But since these systems are generally expensive this was not an option, as one of the aims was to find a method that keeps the costs of biomass measurements down. In addition, techniques including NIR (e.g. when studying the correlation between NDVI and biomass on rangelands) have shown ambiguous results. For example, Diouf (2001) concluded that due to large interannual variations in the strength and parameters of the relationship between biomass and NDVI, NDVI cannot serve as a robust proxy variable for biomass in the Sahel. Also Rosema (1998) investigated this relationship when carrying out a study in Burkina Faso. It was found that the correlation between dry ground biomass and Meteosat derived biomass (MDB) using the visual and IR channel did not represent ground data very well ($R^2$ = 0.45), but at least MDB represents biomass better than the National Oceanic and Atmospheric Administration-NDVI (NOAA-NDVI), which Rosema's data was also compared to. On the other hand, there are studies supporting the inclusion of NIR in biomass estimations (e.g. Edirisinghe, 2011; Al-Bakri & Taylor, 2003 and Lo Seen et al. 1995). Edirisinghe (2011), for instance, observed a clear linear relationship ($R^2$ = 0.82) when NDVI was regressed against biomass on pastures in Western Australia.

One large drawback using images in this manner is that only outgoing radiation has been considered. If incoming radiation would have been taken into account, reflectance could have been estimated and would have offered RGB-values that were not depending on whether the incoming radiation was high or low at the very photo-occasion. Higher incoming radiation naturally leads to higher radiation being reflected from the ground. Therefore, images taken at sunnier occasions have higher values in RGB.

## 5.3 Unsupervised classification

The unsupervised classification was only visually interpreted for some points. However, unsupervised classification seems to encounter the same problems as the GV's; bare ground is not consistently included in one group but falls either into grass or bare ground. This problem is probably larger for yellowing grasses and shadowed/unshadowed bare ground, which endorses the use of NIR. Classifying the images into more than two classes would perhaps have been better at distinguishing grass from bare soil. Nevertheless, unsupervised classification is, just like GV's, only a 2-dimensional representation of the ground and judging from the results for GV's, grass height, LAI and unsupervised classification itself, height needs to be included (or rather treated separately) in order to reflect AGB in these areas.

## 5.4 Grass height

Grass height seems to be the better option when estimating biomass on these grasslands (see figure 12). The reason for grass height seeming to be a better option than using GV's is probably due to the reduced chlorophyll content at the end of the growing season, while the conversion of $CO_2$ and $H_2O$ to carbohydrates continues. Thereby the grass continues to grow despite the yellowing process. If compared to the study by Edirisinghe (2011), the performance is almost as good as traditional measurements and definitely cheaper since the method is quick, could be performed by anyone and the only utensil needed is a scale. A drawback is that the method is not as objective as using DCI’s or satellite images, as the person performing the measurements to some extent needs to make a judgment on the grass height. But according to the results of this study it could be considered suitable as a direct estimation of biomass, especially as the vegetation over this area is very homogeneous.

Indeed, grass height has been proven to correlate well with biomass in other studies. Salas Fernandez et al. (2009) concluded that plant height was one of the most important yield components when studying maize (*Zea mays*) ($r^2 > 0.73$) and sorghum (*Sorghum bicolor*) ($r^2 > 0.68$) as a source of bioenergy in the Midwestern and central plains of the U.S. A slightly weaker correspondence was found for semi-desert grasses in rangelands of the Southwestern U.S., where grass height accounted for 57-72 % of the variation in AGB (Nafus, 2009). But for the study conducted by Nafus (2009), 80-91 % of the variation could rather be explained by grass basal diameter.

The relationship between grass height and biomass should be further investigated and tested over larger areas and several years before any conclusions can be drawn regarding grass height as a variable for calibrating satellite derived biomass. However, the findings in this study remain interesting and could maybe serve as a basis for further research within the area.

## 5.5 LAI

Satellite derived LAI, which is based on spectral properties of the ground, covers a larger area than the sample site, it also includes trees on the site. These have not been taken into account here as the study focuses on grass. However, satellite derived LAI cannot completely follow the increase in biomass. LAI turned out to dip when biomass was still increasing and therefore suggest that measuring reflectance instead of the radiance on the plots would still not have given a condition where RGB images could have served as a replacement or aid in biomass estimation in this area. The similar curves of LAI and the indices also indicates that despite radiance is what is being measured in the DCI’s, the properties described in the reflectance curve should not be neglected. That is; reflectance and DN show a similar pattern at the same wavelength in this case.

# 6. Conclusions

- Estimating AGB on grasslands in Dahra, Senegal using the visible part of the spectrum in DCI's does not seem to give good enough AGB estimations. The correlation between traditional biomass measurements and the applied image analysis techniques is too weak as the indices are unable to distinguish yellowing grass from soil, and shadows can be classified as either soil or grass.

- The unsupervised image classification seems to encounter the same problem as the indices; yellow grass can be treated as bare soil as well as green grass. Moreover, shadowing can cause a discrepancy as to whether how a certain feature should be classified.

- In order to cover a larger region such as the whole Sahel, or at least a substantially larger area of western Sahel, grass heights seem to give the best estimate of AGB. Less accurate AGB measurements covering a large area can in some cases be preferred to more accurate biomass measurements that only cover a very distinct area. However, if grass height derived AGB estimations are considered applicable; more studies on the topic would most likely be needed before extending these types of measurements to other areas.

- Developing a model for calibration of satellite images through grass height measurements lies beyond the scope of this thesis. But after collection of grass height data from several years and larger areas, it is believed that this relationship should be further investigated in order to render an appropriate model that can be used for remotely sensed biomass estimations.

# 7. References

## Litteratura:


Al-Bakri, J.T., Taylor, J.C. 2003. *Application of NOAA AVHRR for monitoring vegetation conditions and biomass in Jordan*. Journal of Arid Environments **54**(3):579-593.

Asner, G.P. 1998. *Biophysical and Biochemical Sources of Variability in Canopy Reflectance.* Remote Sensing of Environment **64**: 234-253.

Boschetti, M., Bocchi, S., Brivio, P.A. 2007. *Assessment of pasture production in the Italian Alps using spectrometric and remote sensing information.* Agriculture, Ecosystems and Environment **118**:267-272.

Chapin, F.S., Matson, P.A., Moonet, H.A. 2002. *Principles of Terrestrial Ecosystem Ecology*. New York, NY. Springer Science Business Media, Inc. Pp. 97-114, 138-141, 384. ISBN: 0-387-95443-0.

Crimmins, M.A, Crimmins, T.M. 2008. *Monitoring Plant Phenology Using Digital Repeat Photography*. Environmental Management **41**:949-958.

Cornforth, R. 2012. *Overview of the West African Monsoon 2011*. Weather **67**(3):59-65.

Desalew, T., Tegegne, A., Nigatu, L., Teka, W. 2010. *Rangeland condition and feed resources in Metema District, North Gondar Zone, Amhara Region, Ethiopia.* IPMS (Improving Productivity and Market Success) of Ethiopian Farmers Project. Working Paper 25. Nairobi, Kenya, ILRI.

Diallo, O., Diouf, A., Hanan, N.P., Ndiaye, A., Prevost, Y. 1991. *Avhrr monitoring of Savanna primary production in Senegal, West Africa – 1987-1988*. International Journal of Remote Sensing **12**(6):1259-1279.

Diouf, A., Lambin, E.F. 2001. *Monitoring land-cover changes in semi-arid regions: remote sensing data and field observations in the Ferlo, Senegal*. Journal of Arid Environments **48**: 129-148.

Edirisinghe, A. 2011. *Quantitative mapping of pasture biomass using satellite imagery*. International Journal of Remote Sensing **32** (10): 2699-2724.

Fensholt, R., Sandholt, I., Stinsen, S. 2006. *Evaluating MODIS, MERIS, and Vegetation Indices Using In Situ Measurements in a Semiarid Environment*. IEEE Transactions on Geoscience and Remote Sensing **44** (7): 1774-1786.

Gessner, U., Niklaus, M., Kuenzer, C., Dech, S. 2013. *Intercomparison of Leaf Area Index Products for a Gradient of Sub-humid to Arid Environments in West Africa*. Remote Sensing **5**:1235-1257.

Giannini, A., Saravanan, Chang, P. 2003. *Oceanic Forcing of Sahel Rainfall on Interannual to Interdecadal Time Scales.* Science **302**:1027-1030.

Gitelson, A.A., Kaufman, Y.J., Stark, R., Rundquist, D. 2002. *Novel algorithms for remote estimation of vegetation fraction*. Remote Sensing of Environment **80**:76-87.

Hein, L., De Ridder, N. 2006. *Desertification in the Sahel: a reinterpretation*. Global Change Biology **12**:751-758.

Herrmann, S.M., Anyamba A., Tucker C.J. 2005. *Recent trends in vegetation dynamics in the African Sahel and their relationship to climate*. Global Environmental Change **15**: 394-404.

Herrmann, S.M., Tappan, G.G. 2013. *Vegetation Impoverishment despite greening: A case study from central Senegal.* Journal of Arid Environments **90**:55-66.

Hickler, T., Eklundh, L., Seaquist, J.W., Smith, B., Ardö, J., Olsson, L., Sykes, M.T., Sjöström, M. 2005. *Precipitation controls Sahel greening trend*. Geophysical Research Letters **32**:L21415.

Hiernaux, P., Mougin, E., Diarra, L., Soumaguel, N., Lavenu, F., Tracol, Y., Diawara M. 2009. *Sahelian rangeland response to changes in rainfallover two decades in the Gourma region, Mali*. Journal of Hydrology **375** (1-2): 114-127.

Hirata M., Oishi K., Marumatu K., Xiong Y., Kaihotu I., Nishiwaki A., Ishida J., Hirooka, H., Hanada M., Toukura Y., Hongo A. 2007. *Estimation of plant biomass and plant water mass through dimensional measurements of plant volume in the Dund-Govi Province, Mongolia*. Japanese Society of Grassland Science ISSN1744-6961.

Huber, S., Fensholt, R., Rasmussen, K. 2011. *Water availability as the driver of vegetation dynamics in the African Sahel from 1982 to 2007.* Global and Planetary Change **76**: 186-195.

Lebourgeois, V., Bégué, A., Labbé, S., Mallavan, B., Prévot, L., Roux, B. 2008. *Can Commercial Digital Cameras Be Used as Multispecral Sensors? A Crop Monitoring Test.* Sensors **8**:7300-732.

Liu, W.T., Xie, X., Katsaros, K.B. 2012. *Observation of oceanic origin of Sahel precipitation from space*. Remote Sensing of Environment **123**: 593-599.

Lillesand, T.M., Kiefer, R.W., Chipman, J.W. 2008. *Remote Sensing and Image Interpretation*. Danvers, MA. John Wiley & Sons. 6th ed. Pp.6, 23, 38. ISBN: 978-0-470-05245-7.

Mishra, A.K., Singh, V.P. 2010. *A review of drought concepts.* Journal of Hydrology **391**(1-2):202-216.

Moulin, C., Chiapello, I.2006. *Impact of human-induced desertification on the intensification of Sahel dust emission and export over the last decades.* Geophysical Research Letters **33**(18):1-5.

Myneni, R.B., Asrar, G. 1994. *Atmospheric Effects and Vegetation Indices*. Remote Sensing of Environment **47**:390-402.

Nafus, A.M., McClaran, M.P., Archer, S.R., Throop, H.L. 2009. *Multispecies Allometric Models Predict Grass Biomass in Semidesert Rangeland.* Rangeland Ecology & Management **62**(1):68-72.

Nicholson, S. 2005. *On the question of the "recovery" of the rains in the West African Sahel*. Journal of Arid Environments **63**:615-641.

Nicholson, S. 2009. *A revised picture of the structure of the "monsoon" and land ITCZ over West Africa.* Climate Dynamics **32**:1155-1171.

Parton, W., Tappan, G., Ojima, D., Tschakert, P. 2004. *Ecological impact of historical and future land-use patterns in Senegal*. Journal of Arid Environments **59**:605-623.

Perez, F., De Stefano, M., Disabato, F., Vigna, R. 2012. *The ITHACA Early Warning System for drought monitoring:first prototype test for the 2010 Sahel crisis.* Italian Journal of Remote Sensing **44**(1):181-195.

Powell, J.M., Fernhdez-Rivera, S., Hiernauxh, P., Turner, M.D. 1996. *Nutrient Cycling in Integrated Rangeland/Cropland Systems of the Sahel*. Agricultural Systems **52**:143-170.

Rautiainen, M., Heiskanen, J., Eklundh, L., Mõttus, M., Lukes, P., Stenberg. P. 2010. *Ecological applications of physically based remote sensing methods*. Scandinavian Journal of Forest Research **25**:325-339.

Reeves, M.C., Zhao, M., Running, S.W. 2006. *Applying Improved Estimates of MODIS Productivity to Characterize Grassland Vegetation Dynamics.* Rangeland Ecology and Management **59**(1):1-10.

Reid, K.D., Wilcox, B.P., Breshears, D.D., MacDonald, L. 1999. *Runoff and erosion in a pinon-juniper woodland: Influence of vegetation patches*. Soil Science Society of America Journal **63**(6):1869-1879.

Ren, H., Zhou, G., Zhang, X. 2011.*Estimation of green aboveground biomass of desert steppe in Inner Mongolia based on red-edge reflectance curve area method.* Biosystems engineering **109**:385-395.

Richardson, A.D., Jenkins, J.P., Braswell B.H., Hollinger D.Y., Ollinger, S.V., Smith, M-L. 2007. *Use of digital webcam images to track spring green-up in a deciduous broadleaf forest*. Oecologia **152**:323-334.

Rosema, A. 1993. *Using METEOSAT for Operational Evapotranspiration and Biomass Monitoring in the Sahel Region*. Remote Sensing of Environment **46**: 27-44.

Salas Fernandez, M.G., Becraft, P.W., Yin, Y., Lübberstedt, T. 2009. *From dwarves to giants? Plant height manipulation for biomass yield*. Trends in Plant Science **14** (8):454-461.

Scurlock, J.M.O., Johnson, K., Olson, R.J. 2002. *Estimating net primary productivity from grassland biomass dynamics measurements*. Global Change Biology **8**:736-753.

Tucker, C.J., Vanpraet, C.L., Sharman, M.J., Van Ittersum, G. 1985. *Satellite Remote Sensing of Total Herbaceous Biomass Production in the Senegalese Sahel: 1980-1984.*Remote Sensing of Envrionment **17**:233.249.

Valenza, J., Diallo, A.K. 1974. Etude des pâturages naturels du nord Sénégal. Etude agrostologique, No 34, IEMVT-LNERV.

Vanamburg, L.K., Trlica, M.J., Hoffer, R.M., Weltz, M.A. 2006. *Ground based digital imagery for grassland biomass estimation*. International Journal of Remote Sensing **27**(5):939-950.

Wang, G., Eltahir, E.A.B. 2000. *Role of vegetation dynamics in enhancing the low frequency variability of the Sahel rainfall*. Water Resources Research **36**:1013-1021.

Westergaard-Nielsen, A. 2010. *Pixelating Plants – Spatial temporal monitoring of phenology and snow cover dynamics in Arctic using unmodified digital cameras*. Master thesis, Institute of Geography and Geology, University of Copenhagen.

Zwiggelaar, R. 1998. *A review of spectral properties of plants and their potential use for crop/weed discrimination in row-crops.* Crop Protection **17:**189-206.

## Web sources:

Au Senegal, 2012:
http://www.au-senegal.com/le-climat-et-la-meteo-du-senegal,046.html?lang=fr
Fetched: 2012-02-23
Updated: 2012

Blue Lobster art and design, 2013:
http://blulob.com/2009/03/08/the-rgb-color-wheel/
Fetched: 2013-07-09
Updated: 2013

CIA (Central Intelligence Agency), "The world factbook", 2013:
https://www.cia.gov/library/publications/the-world-factbook/geos/sg.html
Fetched: 2013-07-03
Updated: 2013-02-21

EROS, 2012:

http://daac.ornl.gov/cgi-bin/MODIS/GLBVIZ_1_Glb/modis_subset_order_global_col5.pl
Fetched: 2012-04-21
Updated:2012-03-07

FAO Stat, 2013:
http://faostat.fao.org/site/612/DesktopDefault.aspx?PageID=612#ancor
Fetched: 2013-07-03
Updated: 2013-01-16

GraphPad Software, 2005:
http://graphpad.com/quickcalcs/pvalue1.cfm?CFID=21492968&CFTOKEN=63b1be725e1f2db0-D639A65D-1A4B-0BEA-813AA494A16AEF56
Fetched: 2012-02-14
Updated: Unknown

Mathworks, 2013:
http://www.mathworks.se/help/stats/examples/cluster-analysis.html
Fetched: 2013-05-15
Updated:2013

NASA, 2011:
http://landsathandbook.gsfc.nasa.gov/data_properties/
Fetched: 2011-12-01
Updated:2011-03-11

NASA, 2013:
http://modis.gsfc.nasa.gov/about/specifications.php
Fetched: 2013-05-15
Updated: Unknown

Töttrup, C., Helldén, U. DeSurvey-IP, 2007:
http://www.comap.ca/kmland/kmland/content/VRCPR/LADA/DeSurvey_1.html
Fetched: 2013-05-15
Updated: Unknown

## Programs:

Clark Labs. IDRISI Andes.
MathWorks. Matlab.

**Institutionen för naturgeografi och ekosystemvetenskap, Lunds Universitet.**

Student examensarbete (Seminarieuppsatser). Uppsatserna finns tillgängliga på institutionens geobibliotek, Sölvegatan 12, 223 62 LUND. Serien startade 1985. Hela listan och själva uppsatserna är även tillgängliga på LUP student papers (www.nateko.lu.se/masterthesis) och via Geobiblioteket (www.geobib.lu.se).

The student thesis reports are available at the Geo-Library, Department of Physical Geography and Ecosystem Science, University of Lund, Sölvegatan 12, S-223 62 Lund, Sweden. Report series started 1985. The complete list and electronic versions are also electronic available at the LUP student papers (www.nateko.lu.se/masterthesis) and through the Geo-library (www.geobib.lu.se).

260 Min Wang (2012) Seasonal and inter-annual variability of soil respiration at Skyttorp, a Swedish boreal forest

261 Erica Perming (2012) Nitrogen Footprint vs. Life Cycle Impact Assessment methods – A comparison of the methods in a case study.

262 Sarah Loudin (2012) The response of European forests to the change in summer temperatures: a comparison between normal and warm years, from 1996 to 2006

263 Peng Wang (2012) Web-based public participation GIS application – a case study on flood emergency management

264 Minyi Pan (2012) Uncertainty and Sensitivity Analysis in Soil Strata Model Generation for Ground Settlement Risk Evaluation

265 Mohamed Ahmed (2012) Significance of soil moisture on vegetation greenness in the African Sahel from 1982 to 2008

266 Iurii Shendryk (2013) Integration of LiDAR data and satellite imagery for biomass estimation in conifer-dominated forest

267 Kristian Morin (2013) Mapping moth induced birch forest damage in northern Sweden, with MODIS satellite data

268 Ylva Persson (2013) Refining fuel loads in LPJ-GUESS-SPITFIRE for wet-dry areas - with an emphasis on Kruger National Park in South Africa

269 Md. Ahsan Mozaffar (2013) Biogenic volatile organic compound emissions from Willow trees

270 Lingrui Qi (2013) Urban land expansion model based on SLEUTH, a case study in Dongguan City, China

271 Hasan Mohammed Hameed (2013) Water harvesting in Erbil Governorate, Kurdistan region, Iraq - Detection of suitable sites by using Geographic Information System and Remote Sensing

272 Fredrik Alström (2013) Effekter av en havsnivåhöjning kring Falsterbohalvön.

273 Lovisa Dahlquist (2013) Miljöeffekter av jordbruksinvesteringar i Etiopien

274 Sebastian Andersson Hylander (2013) Ekosystemtjänster i svenska agroforestrysystem

275 Vlad Pirvulescu (2013) Application of the eddy-covariance method under the canopy at a boreal forest site in central Sweden

276 Malin Broberg (2013) Emissions of biogenic volatile organic compounds in a Salix biofuel plantation – field study in Grästorp (Sweden)

277 Linn Renström (2013) Flygbildsbaserad förändringsstudie inom skyddszoner längs vattendrag

278 Josefin Methi Sundell (2013) Skötseleffekter av miljöersättningen för natur- och kulturmiljöer i odlingslandskapets småbiotoper

279 Kristín Agustsdottír (2013) Fishing from Space: Mackerel fishing in Icelandic waters and correlation with satellite variables

280 Cristián Escobar Avaria (2013) Simulating current regional pattern and composition of Chilean native forests using a dynamic ecosystem model

281 Martin Nilsson (2013) Comparison of MODIS-Algorithms for Estimating Gross Primary Production from Satellite Data in semi-arid Africa

282 Victor Strevens Bolmgren (2013) The Road to Happiness – A Spatial Study of Accessibility and Well-Beingin Hambantota, Sri Lanka

283 Amelie Lindgren (2013) Spatiotemporal variations of net methane emissions and its causes across an ombrotrophic peatland - A site study from Southern Sweden

284 Elisabeth Vogel (2013) The temporal and spatial variability of soil respiration in boreal forests - A case study of Norunda forest, Central Sweden

285 Cansu Karsili (2013) Calculation of past and present water availability in the Mediterranean region and future estimates according to the Thornthwaite water-balance model

286 Elise Palm (2013) Finding a method for simplified biomass measurements on Sahelian grasslands

287 Manon Marcon (2013) Analysis of biodiversity spatial patterns across multiple taxa, in Sweden